Revista de Metalurgia 61 (2)
April-June 2025, e283
ISSN-L: 0034-8750, eISSN: 1988-4222
https://doi.org/10.3989/revmetalm.e283.1716

Optimization of pure aluminum powder metallurgy compacts with ultra-high frequency induction sintering: Duration, energy, and mechanical performance analysis

Hayrettin Gökozan[a], Mehmet Taştan[a], Uğur Çavdar[b,*]

[a] Manisa Celal Bayar University, Turgutlu Vocational School, Department of Electric, 45400, Manisa, Turkey
[b] Izmir Demokrasi University, Engineering Faculty, Mechanical Engineering Department, 35140, Izmir, Turkey
(*Corresponding author: ugur.cavdar@idu.edu.tr)

Submitted: 4 October 2025; Accepted: 12 December 2025; Available On-line: 26 January 2026

ABSTRACT: This study compared the efficacy of Ultra-High Frequency Induction Sintering (UHFIS) against conventional furnace sintering for the production of pure aluminum Powder Metallurgy (PM) compacts. The comparison was based on parameters such as cost, energy consumption, process time, density, and hardness. The UHFIS process was performed using a 2.8 kW, 900 kHz system at 600 °C for six different durations (1 to 10 min). Conventional sintering, conversely, lasted 60 min at 600 °C. The results demonstrated that an increase in UHFIS duration led to a linear rise in energy consumption and cost. However, a 5-minute UHFIS duration was observed to optimize hardness and density values while keeping costs controlled. The UHFIS method provided a significant advantage by reducing the process time by a factor of 12 compared to conventional sintering. Conversely, due to its lower energy consumption, conventional furnace sintering offered a cost that was three times lower than UHFIS. In conclusion, the shorter process time and increased production capacity effectively compensate for the higher costs of UHFIS. With an optimized sintering duration, the UHFIS method exhibits significant potential for the efficient and economical production of high-quality aluminum PM compacts in industrial and mass production settings.

KEYWORDS: Al; Conventional sintering; Energy consumption; Energy cost; Induction sintering; PM

Citation/Citar como: Gökozan, H.; Taştan, M.; Çavdar, U. (2025). "Optimization of pure aluminum powder metallurgy compacts with ultra-high frequency induction sintering: Duration, energy, and mechanical performance analysis". *Rev. Metal.* 61(2): e283. https://doi.org/10.3989/revmetalm.e283.1716

RESUMEN: *Optimización de compactos de pulvimetalurgia de aluminio puro mediante sinterización por inducción de ultraalta frecuencia: Análisis de duración, energía y rendimiento mecánico.* Este estudio comparó la eficacia de la sinterización por inducción de ultraalta frecuencia (UHFIS) con la sinterización en horno convencional para la producción de compactos de pulvimetalurgia de aluminio puro (PM). La comparación se basó en parámetros como coste, consumo energético, tiempo de proceso, densidad y dureza. El proceso UHFIS se realizó con un sistema de 2,8 kW y 900 kHz a 600 °C durante seis duraciones diferentes (de 1 a 10 min). La sinterización convencional, por otro lado, duró 60 min a 600 °C. Los resultados demostraron que un aumento en la duración del UHFIS condujo a un aumento lineal del consumo energético y el coste. Sin embargo, se observó que una duración del UHFIS de 5 minutos optimizaba los valores de dureza y densidad, manteniendo los costes bajo control. El método UHFIS proporcionó una ventaja significativa al reducir el tiempo de proceso 12 veces en comparación con la sinterización convencional. Por el contrario, debido a su menor consumo energético, la sinterización en horno convencional ofrecía un coste tres veces inferior al de la sinterización por inducción ultra alta (UHFIS). En conclusión, la reducción del tiempo de proceso y la mayor capacidad de producción compensan eficazmente los mayores costes de la UHFIS. Con una duración de sinterización optimizada, el método UHFIS presenta un potencial significativo para la producción eficiente y económica de compactos de PM de aluminio de alta calidad en entornos industriales y de producción en masa.

Copyright: © 2025 CSIC. This is an open-access article distributed under the terms of the Creative Commons Attribution 4.0 International (CC BY 4.0) License.

PALABRAS CLAVE: Al; Consumo energético; Coste energético; Sinterización por inducción; Sinterización convencional; PM

ORCID: Hayrettin Gökozan (https://orcid.org/0000-0002-8917-4001); Mehmet Taştan (https://orcid.org/0000-0003-3712-9433); Uğur Çavdar (https://orcid.org/0000-0002-3434-6670)

1. INTRODUCTION

Aluminum materials are widely used today due to their properties such as lightness, superior mechanical strength, and corrosion resistance (Durmuş *et al.*, 2020; Parasuraman *et al.*, 2022; Teker *et al*., 2023). Many industries, including automotive, aerospace, electronics, and construction, benefit from these advantages of aluminum. The lightweight nature of aluminum is particularly preferred in the automotive industry to enhance fuel efficiency. Additionally, its corrosion resistance and durability ensure long life and reliability in structural applications. In this context, numerous studies have been conducted to explore the properties and application areas of aluminum materials. In this study, aluminum PM materials were used to evaluate the effects of different sintering methods. Conventional furnace sintering, while providing homogeneous properties, can impose limitations on productivity in mass production due to long processing times and lead to high energy consumption (Gül *et al.*, 2020; Borges *et al.*, 2023). This situation increases the interest in faster and more energy-efficient sintering methods (Wu *et al.*, 2024). PM is a crucial technique used in the production of both semi-finished and finished products. This method involves mixing metal powders, compressing them into a mold, and heating them below their melting point to achieve the desired properties (Angelo P.C., 2008). PM offers advantages in the production of complex-shaped parts and minimizes material waste. Additionally, materials produced using this method possess a homogeneous microstructure and controlled porosity levels, which are critical for various industrial applications. Sintering is one of the critical stages of PM, (Furlan *et al.*, 2017; Ozer *et al.*, 2024) and it involves heating the particles at temperatures below their melting point to bond them together, thereby enhancing mechanical strength (Ge *et al.*, 2017) . During sintering, atomic diffusion mechanisms (surface, grain boundary, and volume diffusion) become active, promoting the formation and growth of 'necks' between particles, which leads to a reduction in porosity and densification of the compact. This process directly influences the final mechanical properties of the material (Lu *et al.*, 2021). PM compacts can be sintered using various methods, such as atmosphere-controlled furnaces, medium-frequency induction systems (Çavdar, U. *et al.,* 2014) and UHFIS, (Çavdar, P. and Çavdar, U., 2015; Gokozan *et al.*, 2016). Induction sintering allows for more controlled changes in the microstructure due to its rapid heating and cooling capability, whereas conventional sintering enables more homogeneous properties over longer durations. Induction systems can be employed in various processes, including heat treatment (Taştan *et al.*, 2015, Taştan *et al.*, 2020) welding (Çavdar and Gülşahin, 2014), casting, and forging (Çavdar, 2014).

Induction-based sintering is increasingly utilized across industries due to the distinct advantages it offers over conventional furnace sintering. The indirect induction approach for sintering parts produced by Material Extrusion Additive Manufacturing (MEAM) significantly reduces processing times and energy consumption by eliminating transport steps and cutting cycles that previously required hours down to minutes, thereby boosting the efficiency of the production flow (Varela De Seijas *et al.*, 2023; Vilchez *et al.*, 2023). In lightweight structural alloys, such as powder metallurgy titanium systems, induction heating promotes accelerated densification kinetics, which facilitates reaching the high relative densities required for aerospace and biomedical applications. The ability to rapidly tailor temperature profiles also enables precise control over grain growth during consolidation, ensuring the repeatability of production and tight control of final mechanical properties (Pan *et al.*, 2024). For hard-metal and tool-steel applications (Teslia *et al.*, 2024), rapid induction sintering strategies achieve high-density and controlled microstructures within shortened processing times, yielding superior cutting tools and wear-resistant components (Fei *et al.*, 2021). Furthermore, in electronic packaging, the inductive sintering of silver microparticles utilizes local heating to confine energy to the bond region. This process produces strong die-attach joints at comparatively low bulk temperatures, successfully shortening cycle times (Rochala *et al.*, 2023). Consequently, induction sintering stands out for its rapid heating/cooling cycles, local energy delivery, improved energy efficiency, and ease of integration into continuous production lines. These combined benefits position induction sintering as a superior alternative to conventional methods in both research and industrial PM workflows (Ruiz-Esparza-Rodríguez *et al.*, 2022).

The sintering of powders in PM can be performed using different techniques. For instance, the Spark Plasma Sintering (SPS) method, (Chang *et al.*, 2017; Jeong *et al.*, 2017; Kozhakhmetov *et al.*, 2021; Alipour *et al.*, 2024) is similar to the hot uniaxial pressing method, where high pressure and direct current (DC) are applied to the powders within the mold. The conventional sintering method, (Raihanuzzaman *et al.*, 2015; Yang *et al.*, 2016) is performed in furnaces where

atmosphere, temperature, and duration are carefully controlled. Microwave Sintering (MS) (Ghobadi *et al.*, 2017; Reddy *et al.*, 2017) is used for sintering samples at higher heating rates and shorter waiting times, allowing for the production of finer grain structures compared to pressureless sintering. In recent years, other advanced sintering techniques such as SPS (Nisar *et al.*, 2021), MS (Dwivedi *et al.*, 2024) and laser sintering (Junqueira *et al.*, 2025) have also been investigated. These methods offer rapid heating rates and short processing times, providing potential advantages in terms of microstructural control and energy efficiency (Zuo *et al.*, 2025). In this study, the aluminum powders used had a purity of 99.9% and particle sizes ranging from 45 to 106 µm, providing a homogeneous microstructure. The powders were prepared by mixing them for an optimal duration and pressing them under pressure to form the samples. This study comprehensively examines the effects of different sintering durations and methods on aluminum PM materials, particularly focusing on the energy consumption and cost analysis of the induction sintering method. While previous research has emphasized the critical impact of sintering durations on microstructural properties, this study also considers the economic efficiency of induction sintering (Çavdar, U. and Atik, E.,2014).

2. MATERIALS AND METHODS

In this study, pure Al PM compacts were prepared using aluminum powders with particle sizes ranging from 45 to 106 µm. The samples were processed using two different sintering methods; one group was sintered in a batch-type furnace, while the other group was sintered using an induction system. To obtain a homogeneous mixture, the aluminum powders were mixed in a V-Type mixer at a speed of 20 revolutions per minute. After mixing, cold pressing was performed at 300 MPa using a "Hidropar" branded uniaxial press machine. The dimensions of the obtained PM compacts were specified as follows: diameter: 18 mm and height: 2 mm. The first group of samples was sintered using an induction generator operating at a frequency of 900 kHz and a power of 2.8 kW. UHFIS is based on the principle that an alternating magnetic field, created by applying an alternating voltage to a conductive coil, induces eddy currents within the material (Mishra, 2021). In non-magnetic materials like aluminum, these eddy currents convert directly into heat energy through the electrical resistance (Joule heating) of the material. The heating depth, also known as penetration depth (δ), is related to the material's resistivity (ρ), magnetic permeability (µ), and induction frequency (f) (Ascona García *et al.*, 2025). The ultra-high frequency of 900 kHz used in our study ensures that the heat is concentrated near the surface of the specimen (skin effect), allowing for rapid and efficient heating (Bao *et al.*, 2022). This rapid and internal heat generation significantly shortens the sintering time compared to conventional furnace heating, which relies on slower heat transfer from the outside. The induction temperature was measured using an infrared thermometer integrated into the system and maintained at the desired level. The Al PM compacts were sintered at 600 °C, under a vacuum of 10^{-1} torr, for durations of 1, 2, 3, 4, 5, and 10 minutes with the aid of UHFIS. Sintering under a vacuum environment (10^{-1} torr) minimizes the oxidation of aluminum, providing a purer and more homogeneous sintering atmosphere, which positively affects the mechanical properties of the resulting compacts (Velavan *et al.*, 2021). After sintering, the PM compacts were naturally cooled. The image of the induction system and the implementation of the sintering process on a vacuum environment are shown in Fig. 1a and Fig 1b, respectively.

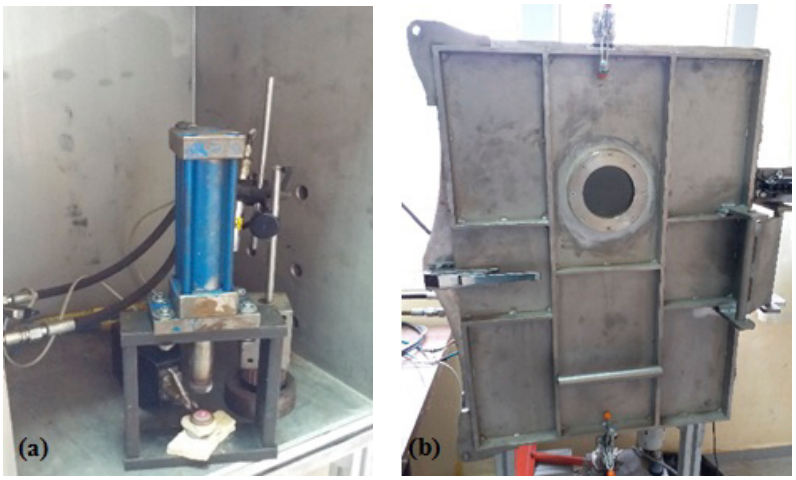

Figure 1. a) The image of the induction system b) Implementation of sintering process on vacuum environment.

The second group of samples was sintered in an open atmosphere furnace at 600°C for 60 minutes using a 2 kW "Proterm" branded chamber furnace. After the sintering process, the PM compacts were naturally cooled in the ambient environment. Figure 2a shows the image of the furnace-sintered Al PM compact, while Fig. 2b displays the image of the non-sintered Al PM compact.

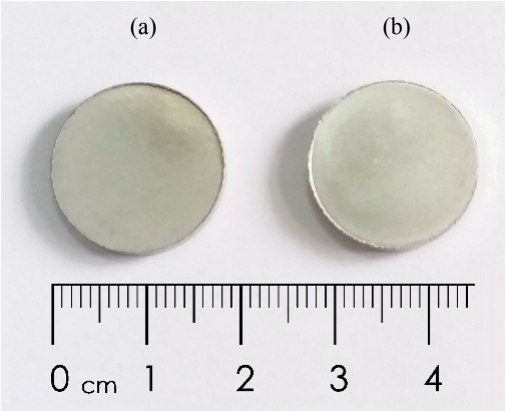

Figure 2. a) Furnace-sintered Al PM compact, and b) Non-sintered Al PM compact.

Figure 3 shows the sintering process of the aluminum PM compact. During the sintering process, an infrared (IR) sensor is used to measure the surface temperature. The IR sensor accurately measures the surface temperature of the compact, allowing for precise control of the sintering process at the desired temperature. This precise temperature control helps optimize the microstructural properties of the compact.

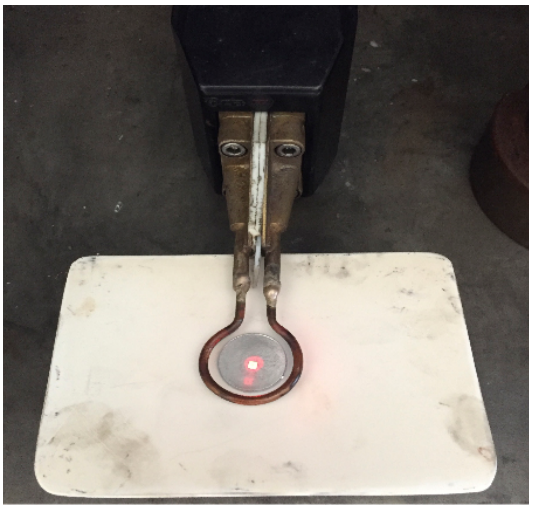

Figure 3. Sintering PM compact with UHFIS.

Figure 4 shows Al PM compacts sintered for different durations using the UHFIS method. The compact in figure 4a has a relatively smoother and denser surface following a 2-minute sintering process. This short-duration process allows partial bonding within the microstructure of the compact, resulting in a uniform surface. The compact in figure 4b exhibits more noticeable densification with a 4-minute sintering duration. Its surface becomes even smoother, and the degree of bonding within the microstructure increases. In Fig. 4c, the effects of a 10-minute sintering duration can be observed. More pronounced roughness and porosity have formed on the surface, indicating the changes in the microstructure caused by the longer sintering time. This demonstrates how sintering at different durations clearly impacts the physical properties of Al PM compacts.

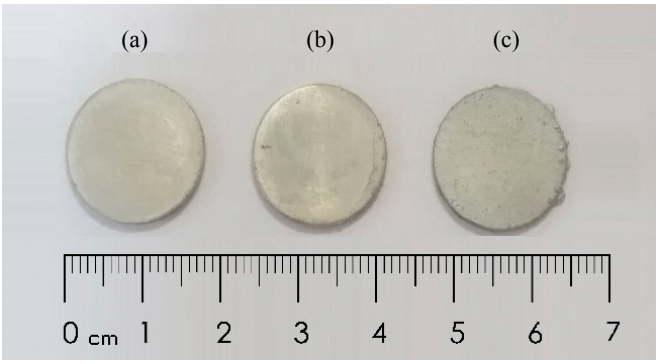

Figure 4. Aluminum PM compacts with UHFIS: a) 2 min, b) 4 min and c) 10 min, sintering images.

The flowchart in Fig. 5 illustrates the entire sintering process of aluminum powders, providing a comparative overview of the two main sintering methods: "Induction Sintering" and "Conventional Sintering". In the first stage, aluminum powders are mixed homogeneously using a V-type mixer. This process ensures the proper distribution of the powders and prepares them for the subsequent sintering stages. The mixed aluminum powders are then cold-pressed into Al PM compacts. In the induction sintering process, the pressed Al PM compacts are sintered at 600 °C for different durations (1, 2, 3, 4, 5, and 10 min). After each sintering process, a natural cooling phase is applied. In the conventional sintering process, the compacts are sintered at 600 °C for 60 min, followed by natural cooling. The hardness measurement of PM compacts was conducted using the Brinell hardness test method (Singh, 2021). The hardness measurements of the samples were performed with the TIME TH-140 Digital Hardness Measuring Device (Rojas-Macedo *et al.*, 2024). Hardness values were obtained from 5 different points on each sample, and the results were calculated by averaging this hardness. The relative densities of the compacts were evaluated using the Archimedes Method, (Fu *et al.*, 2023; Mohammadi *et al.*, 2023). For this test, the Radwag AS 220/C/2 Archimedes Scale was used, (Elkilani *et al.*, 2024; Gafur *et al.,* 2023).

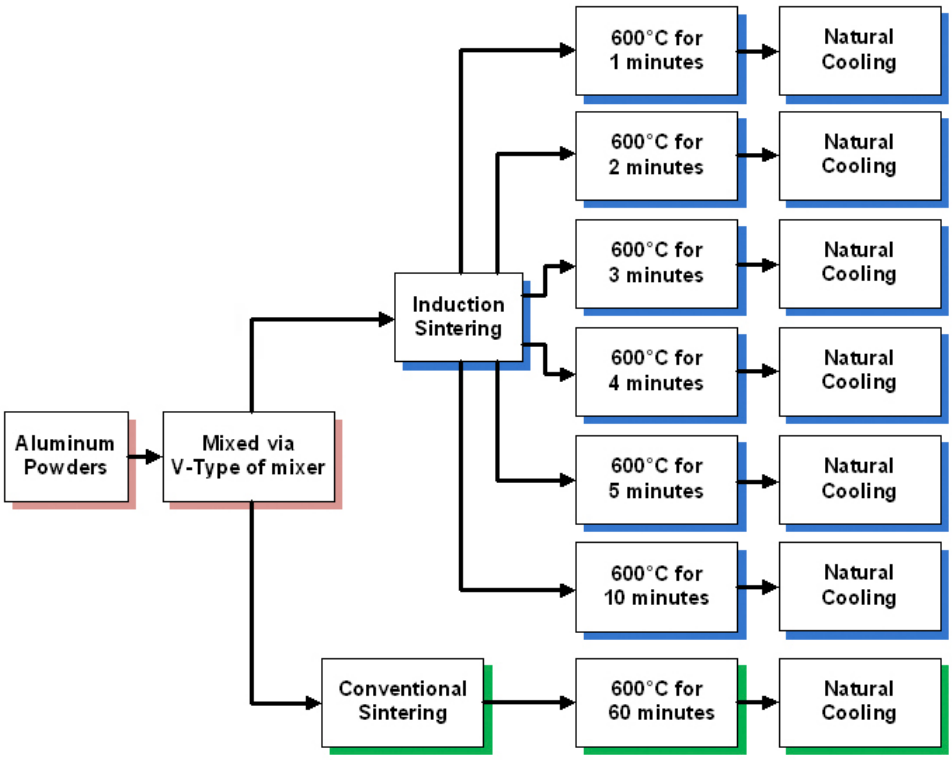

Figure 5. Flow chart of all processes.

Figure 6 shows the key components of the LabVIEW™-based measurement and data acquisition system. This system is designed to measure and analyze critical parameters such as power consumption and power quality of a machine or system. Electrical energy from the power source is measured through voltage and current sensors and relayed to a data acquisition card (DAQ - NI PCI 6221). Data from these sensors is recorded via the LabVIEW™ 8.5 graphical interface and analyzed according to IEC standards . The electrical parameters of the 2.8 kW, 900 kHz UHFIS were collected using this LabVIEW™-based measurement system (Taskin and Gokozan, 2011; Özdemir and Taştan, 2014; Taştan, 2019) The collected data was processed using LabVIEW™ software for power consumption and quality analyses. This configuration enables precise measurement and analysis of electrical parameters, allowing for the evaluation of the energy efficiency and performance of the induction system used in the experiments.

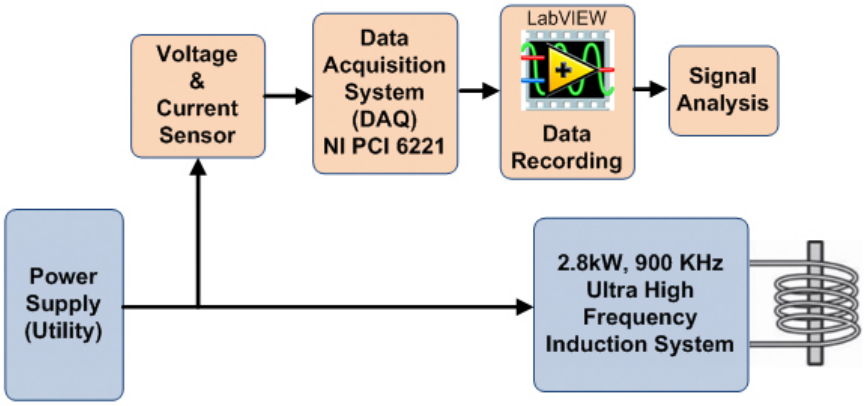

Figure 6. Building block of LabVIEW™-based measuring collecting system.

Finally, a specific sample preparation procedure was followed to perform the microstructural analyses. The samples were consecutively sanded using 180 to 1200 grit sandpaper and subsequently polished with 3-micron and 1-micron diamond solutions via a Metkon Farcipol 1V polishing machine. The polished specimens were then etched with Keller's solution 2.5 ml HNO_3, 1.5 ml HCl, 1 ml HF, 95 ml water) to reveal the microstructure. Metallographic examinations were performed using a Nikon Eclipse LV150N optical microscope.

3. RESULTS AND DISCUSSION

This section presents the experimental results obtained from the induction and conventional sintering processes of pure aluminum PM compacts, followed by a comprehensive discussion of their implications on material properties, energy consumption, and cost. The analysis begins with a detailed examination of the electrical parameters recorded during induction sintering.

The current variation in Fig. 7 shows the different stages of the sintering process and the associated electrical changes occurring within the material's structure. Initial Stage (0-2.5 sec): During this phase, the current exhibits a fluctuating profile with high amplitude. This condition represents the initiation of the induction sintering process, where the effect of the coil's electromagnetic field on the compact is at its peak. At this point, the connections between aluminum powder particles are relatively loose, with numerous voids present. The high current observed during this initial stage is due to the increased energy density within the material's microstructure and the high electrical resistance. The induction current generates eddy currents within the material, resulting in the rapid heating of the compact. Transition Stage (2.5-4 sec): In this phase, a decrease in current amplitude begins. The energy density at the start of the sintering process induces microstructural changes within the material. During this period, atomic diffusion initiates at the contact points between the aluminum particles, forming bonds between them. This process leads to an increase in electrical conductivity and a reduction in overall electrical resistance within the material. Consequently, the current amplitude gradually decreases and stabilizes during this stage. Stable Stage (4-10 sec): At this point, the current reaches a more steady profile. This indicates that the material's microstructure has attained a certain density, and despite the continuation of diffusion processes, the electrical properties of the compact have largely stabilized.

Throughout the sintering process, electrical conductivity remains high, and electrical resistance is relatively low. The free movement of electrons within the material becomes more effortless, resulting in a lack of significant fluctuations in the current. This indicates that the sintering process has entered a stable phase, reflecting the electrical changes associated with the bonds and density formed within the material. In summary, the current variation in Fig. 7 shows the microstructural evolution during the sintering process and demonstrates how the electrical conductivity of the material improves over time. The initially high electrical resistance is due to the gaps and weak contact points between particles in the material. However, as the process advances, this resistance decreases, and the current stabilizes.

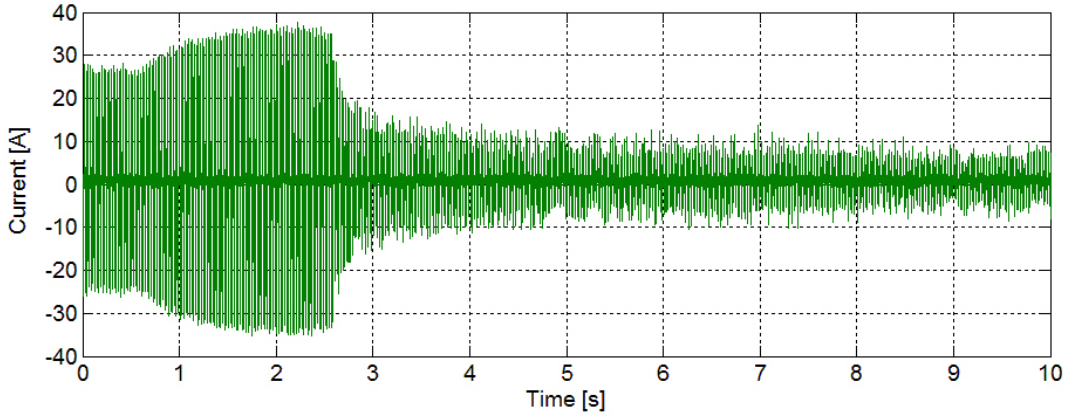

Figure 7. Current change graph for the first 10 sec of the sintering process at 600 °C.

The graph in Fig. 8 shows the variation in power consumption during the first 10 sec of the sintering process conducted at 600 °C. Initially, between 0 and 2.5 sec, the power consumption rapidly increases, reaching approximately 2.5 kW. This increase represents the energy provided by the induction coil to quickly heat the Al PM compact. The heat raises the temperature of the aluminum powders, supplying the necessary energy input for the commencement of the sintering process. At this stage, the high energy consumption is attributed to the rapid heating of the material and the distribution of thermal energy throughout the Al PM compact. The onset of the decrease in power consumption at 2.5 sec indicates that the material is approaching the target temperature rapidly and transitioning into thermal equilibrium. This process continues until approximately 4 sec, during which energy consumption decreases. This observation signifies that the PM compact has begun to maintain its heat rather than storing additional energy. The interval between 4 and 10 sec represents the period during which power consumption stabilizes. From the 4th second onwards, power consumption levels off at around 0.6-0.7 kW. During this phase, as the material remains at the target temperature, energy consumption is maintained at the minimum level required to sustain that temperature. The stable power consumption indicates that the system operates solely to compensate for heat loss, demonstrating that the sintering process has reached a stable state.

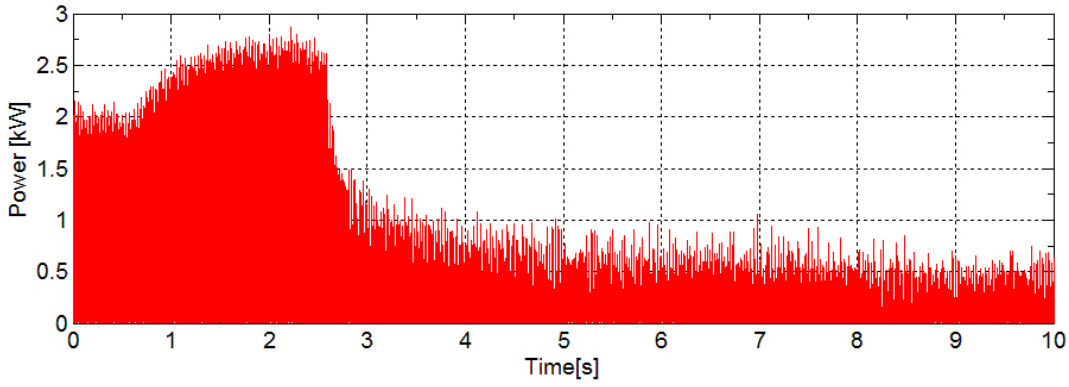

Figure 8. Power change graphic for the first 10 sec of sintering process on 600 °C temperature.

Table 1 summarizes the surface hardness and density values of the PM aluminum compacts produced under various sintering durations. To ensure statistical reliability, experiments were conducted using triplicate samples for each specific induction sintering time (1, 2, 3, 4, 5, and 10 min), as well as for the conventional sintering control group. Measurements were acquired from five distinct locations on each specimen surface-specifically one central point and four peripheral points-to assess homogeneity. Consequently, each presented value represents the overall arithmetic mean derived from these cumulative measurements across the replicate samples, reported alongside the standard deviation to demonstrate process repeatability.

Table 1. HB hardness and density values of aluminium samples

Al Compacts	Induction Sintering, 600 °C						Conventional Sintering 600°C
	1 min	2 min	3 min	4 min	5 min	10 min	60 min
Hardness (HB)	15	26	30	34	36	41	35
SD (HB)	0.23	0.41	0.48	0.50	0.53	0.61	0.52
Density ($g \times cm^{-3}$)	2.054	2.239	2.399	2.450	2.502	2.589	2.475
SD ($g \times cm^{-3}$)	0.040	0.045	0.049	0.050	0.052	0.055	0.050
% Density	75.8	82.6	88.5	90.4	92.3	95.5	91.3

Through conventional methods, a sintering process conducted in an argon atmosphere at 600 °C for 60 min resulted in a hardness of 35 HB and a density of 2.475 $g \cdot cm^{-3}$. The same hardness and density values were achieved using the UHFIS method with a sintering duration of 4-5 min in a vacuum environment, as shown in Fig. 4b. This is consistent with other conventional furnace sintering studies on pure aluminum, where (Avci and Güleç, 2021) documented approximately 40 HV hardness and 2.33 $g \times cm^{-3}$ density after 60 min of sintering at 600 °C. This comparison highlights the efficiency of the UHFIS method, demonstrating that induction sintering durations of approximately 4-5 min yield comparable results to those obtained through the much longer conventional sintering process.

As the sintering time increases, both hardness and density exhibit a noticeable upward trend, indicating an enhancement in material properties. Longer sintering durations allow for more atomic diffusion to occur, supporting these microstructural improvements. Additionally, the data indicate that as the duration of induction sintering increases, the hardness and density values of the aluminum PM compacts also rise. However, analysis of the values confirms that sintering durations of 1-3 min are insufficient for effective sintering and do not allow for adequate bonding of particles within the material. Furthermore, it was determined that a sintering duration of 10 min is outside the optimal range for aluminum PM compacts, as this duration leads to disproportionate energy consumption and potential microstructural degradation relative to the achieved improvement in material properties. Tests conducted during the study revealed that sintering durations exceeding 5 min resulted in localized melting. The finding that a 5-min sintering duration is optimal suggests that sufficient particle bonding and pore closure are achieved within this timeframe. In the literature, high density and hardness values in PM are generally associated with well-sintered microstructures having low porosity and strong inter-particle bonds. For instance, a study by (Leszczyńska-Madej *et al.*, 2019) SPS of pure aluminum compacts reported 28 HB hardness and 97-99% density after 2.5 min of sintering at 580-600 °C. The observed localized melting at 10 min of sintering may be a result of excessive heat input or uneven heat distribution, which typically leads to grain growth and in some cases, degradation of mechanical properties. Although microstructural examination could not be performed, the increased surface roughness and porosity (Fig. 4c) support these potential microstructural changes and show parallels with property degradation caused by over-sintering reported in the literature. In conclusion, when comparing conventional sintering methods to induction sintering, it has been established that the optimal sintering duration for aluminum PM compacts using UHFIS is 5 min. This duration optimizes the material properties while making the process more efficient and time-effective.

Hardness, density, and microstructure analyses revealed that sufficient sintering was not achieved in the 1, 2, and 3-min UHFIS processes. Furthermore, melting was observed during the 10-min induction sintering. Consequently, since the most favorable powder bonding and sintering results were obtained at 4 and 5 min, the microstructural states

of these durations, along with the 10-min UHFIS sample representing the over-sintering region and the conventionally sintered compact, are presented in Fig. 9. An examination of Fig. 9a (4 min) and Fig. 9b (5 min) indicates that these short UHFIS durations lead to an effective sintering reaction within the compacts. These microstructures reveal that the pores have largely become isolated, small, and spherical. This morphology confirms that the densification stage of the sintering process has been successfully completed, achieving the characteristics of the final stage and ensuring strong inter-particle bonding (neck formation). The microstructure resulting from the 5-min UHFIS process (Fig. 9b) exhibits characteristics similar to the microstructural appearance obtained via long-duration (60-min) conventional sintering (Fig. 9d); both tend to display a homogeneous and low-porosity distribution. This visual consistency supports UHFIS's potential to achieve comparable microstructural quality within a significantly shorter processing time than the traditional method.

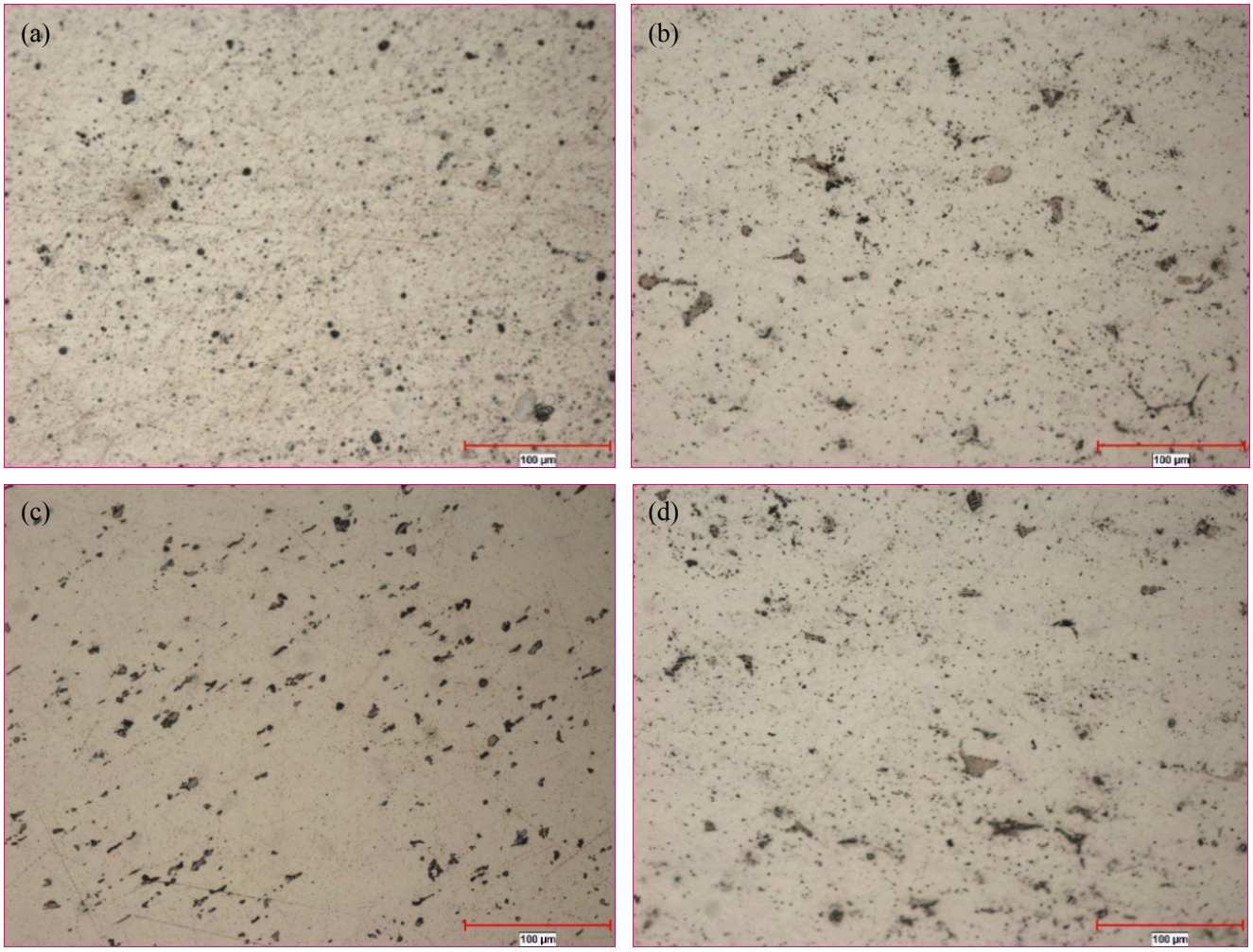

Figure 9. Microstructures of sintered samples with: a) UHFIS Methods for 4 min, b) UHFIS Methods for 5 min, c) UHFIS Methods for 10 min, and d) convensitonal method.

In contrast, the 10-min UHFIS sample presented in Fig. 9c displays noticeable microstructural deviations. In this image, instead of the regular pores observed in the 4 and 5-min samples, the presence of more irregular, partially coalesced, and noticeably larger pores is evident. This condition suggests an over-sintering scenario, where structural integrity begins to degrade due to localized melting initiated by the high energy input over the extended duration. In light of these observations, microstructural analysis indicates that the 5-min UHFIS duration represents the optimal balance for Al PM compacts, providing sufficient bonding and consistent results. When comparing rapid sintering methods that enhance densification, Spark Plasma Sintering (SPS), Microwave Sintering (MS), and Laser Sintering are recognized

as competitors to the UHFIS method. The SPS technique achieves densification within 5–20 min by applying uniaxial pressures at comparatively lower sintering temperatures and relatively mild pressures than other sintering methods. While this technique is effective, the high pressure loading and the requirement for graphite tooling restrict part size and escalate production costs. Microwave Sintering, conversely, provides volumetric heating and operates with cycle times of 10–30 min, though it necessitates careful electromagnetic coupling and the use of susceptors. The heating rates achieved by MS are generally lower than those obtained with SPS or UHFIS. In industrial contexts, the resulting lower heating rates prolong the sintering time, sometimes requiring MS only for specific sintering situations due to its slow heating process. Laser-based sintering or melting processes achieve extremely high localized heating and cooling rates, but their layer-by-layer operation fundamentally limits efficiency for bulk compacts, often resulting in surface roughness on the sintered components.

In contrast, the UHFIS method offers rapid heating and reduced energy consumption, facilitating the complete densification of metallic compacts within 3–10 min using electromagnetic induction flux, and without the necessity for external pressure or relatively complex metal/graphite tooling. Our study specifically determined that a 5-min UHFIS duration for Al PM compacts yields mechanical properties (36 HB hardness and 92.3% density) equivalent to those obtained through 60 min of conventional sintering. Owing to its swift sintering time, interchangeable mold shaping, and the capacity for induction coils to be designed for large metal parts, UHFIS possesses distinct advantages among rapid sintering methods and is consequently positioned as a superior candidate for industrial and mass production.

Table 2 presents a comparative analysis of energy consumption and cost values for aluminum PM compacts utilizing induction and conventional sintering methods. In induction sintering at 600 °C, a significant increase in energy consumption was observed with extended sintering duration. For instance, while 2.670 $kWh \cdot kg^{-1}$ of energy was consumed in 1 min, this value escalated to 6.121 $kWh \cdot kg^{-1}$ at 5 min. A parallel increase was noted in terms of cost, with the 5-min sintering process costing $\$0.5994 \cdot kg^{-1}$. According to the obtained results, 5-minute induction sintering provides optimum mechanical properties for aluminum PM compacts. This demonstrates the feasibility of achieving high performance in a shorter timeframe compared to conventional sintering. Conversely, the conventional sintering process, conducted at the same temperature for 60 min, recorded a lower energy consumption of 1.957 $kWh \cdot kg^{-1}$ and a reduced energy cost of $\$0.1916 \cdot kg^{-1}$. However, this 1-hour process duration substantially diminishes production efficiency. The rapid attainment of target hardness and density via induction sintering, within a shorter duration, consequently reduces total production time, offering cost-effectiveness and time savings in mass production. While conventional sintering exhibits lower energy consumption, its protracted process renders it less efficient on an industrial scale. Therefore, induction sintering emerges as a more suitable industrial method, characterized by its high efficiency and rapid processing capabilities.

Table 2. Power consumption values and costs per kg following the induction sintering and conventional sintering of aluminium samples

Al Compacts	Induction Sintering 600°C						Conventional Sintering 600 °C
	1 minutes	**2 minutes**	**3 minutes**	**4 minutes**	**5 minutes**	**10 minutes**	**60 minutes**
Energy Consumption (kW.kg-1)	2,670	3,364	4,410	5,248	6,121	11,302	1,957
Cost ($.kg-1)	0,2024	0,3294	0,4319	0,5139	0,5994	1,1067	0,1916

Figure 10 illustrates the impact of sintering time on key parameters such as hardness, density, energy consumption, and cost for aluminum PM compacts. As the sintering time increases, both hardness and density exhibit a noticeable upward trend, indicating an enhancement in material properties. Simultaneously, energy consumption and cost rise significantly, highlighting the trade-off between achieving desired mechanical properties and the associated production expenses. This graph reinforces the importance of optimizing sintering duration to balance improved material performance with economic efficiency.

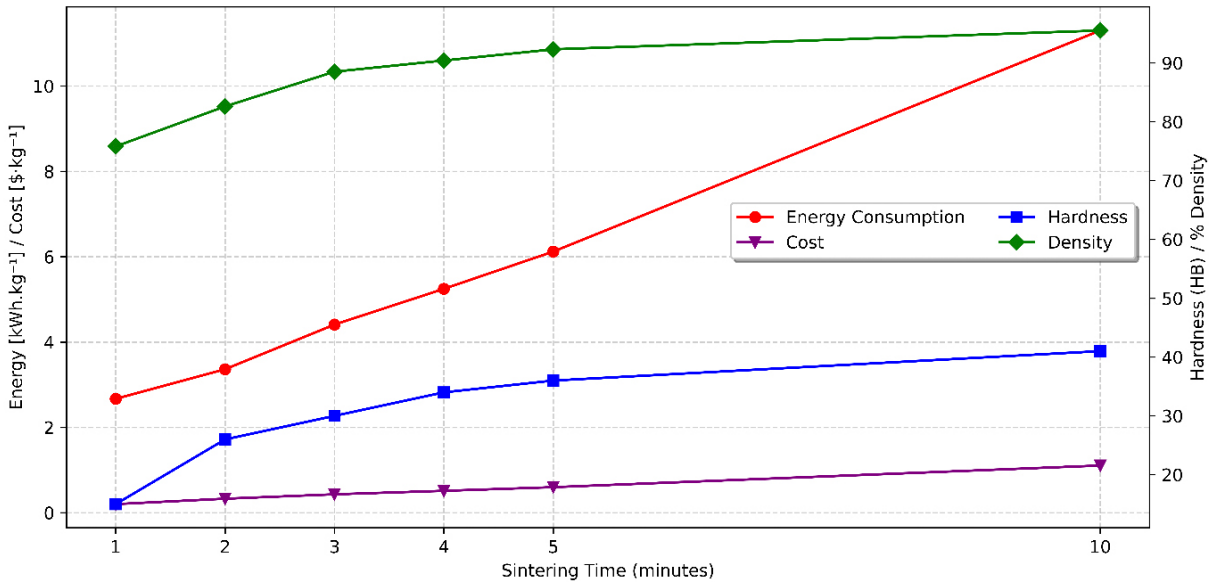

FIGURE 10.

4. CONCLUSIONS

- This study evaluated the comparative performance of UHFIS and conventional sintering methods for sintering pure aluminum PM compacts. The findings elucidate the effects of both methods on cost, energy consumption, process time, density, and hardness. In the induction sintering process, a significant linear increase in energy consumption was observed with the extension of sintering duration from 1 to 10 min; this escalation was paralleled by an increase in production costs. This finding underscores the critical importance of determining the optimal sintering duration to ensure energy efficiency and cost control, particularly in mass production scenarios.

- Experimental analyses revealed that a 5-min induction sintering duration yielded optimal mechanical properties for aluminum PM compacts. During this period, hardness values of 36 HB and a relative density of 92.3% were achieved. This optimized duration facilitates the effective management of energy consumption and production costs. The study observed that extending the sintering duration beyond 5 min led to localized melting and resulted in a disproportionate increase in energy and cost relative to the mechanical improvements obtained. In light of these findings, utilizing a 5-min sintering duration is recommended for industrial production.

- In terms of processing time, the UHFIS method demonstrated a notable advantage over conventional sintering, reducing the sintering duration of Al-based PM compacts by a factor of 12. Although both methods are capable of producing products with comparable mechanical properties, the significantly shorter processing time of induction sintering renders it more appealing for mass production applications. The rapid completion of the sintering process directly enhances production capacity by allowing the manufacturing of a greater number of products within the same timeframe.

- Regarding cost performance, conventional furnace sintering offered approximately three times lower costs than induction sintering, attributed to its reduced energy consumption (1.957 $kWh \cdot kg^{-1}$). However, the lengthy process time of 60 min severely constrains its efficiency in mass production, potentially creating bottlenecks in the production line. Conversely, the initially higher costs associated with induction sintering can be offset by its shorter processing time and accelerated product cycle, thereby holding the potential to reduce overall production costs at an industrial scale.

- In conclusion, despite certain limitations pertaining to energy consumption and cost control, the induction sintering method exhibits substantial potential for industrial and mass production due to its reduced processing

time and enhanced efficiency. Precise determination of the optimal sintering duration can maximize the advantages offered by this method, contributing to the economical production of high-quality products. The achieved optimal mechanical properties and process efficiency position UHFIS competitively among other rapid sintering methods (SPS, laser sintering, and MS), particularly concerning cost-effectiveness and ease of application.

ACKNOWLEDGMENTS

In this study, UHFIS was using for this resarch was ensured by FBE 2012-022 Manisa Celal Bayar University BAP project and 214M414 TUBITAK project.

Declaration of Competing Interest

The authors declare that they have no known competing financial interests or personal relationships that could have appeared to influence the work reported in this paper.

AUTHORSHIP CONTRIBUTION

H. Gökozan: Conceptualization, Methodology, Investigation, Writing-original draft. **M. Taştan:** Conceptualization, Methodology, Formal analysis, Data curation, Writing-review and editing. **U. Çavdar:** Supervision, Project administration, Resources.

REFERENCES

Alipour, M., Ardestani, M., Moazami-Goudarzi, M. (2024). Chemical synthesis, characterization and spark plasma sintering of Cu and Cu/TiO_2 composite powders. *Sci. Sinter.* 56 (3), 335–347. https://doi.org/10.2298/SOS231204003A.

Angelo P.C., Subramanian, R. (2008). *Powder metallurgy: Science, Technology and Applications*. Eastern Economy Edition, New-Delhi, pp. 131–133.

Ascona García, P.P., Ordoñez Carpio, G.E., Zelada Zamora, W.M., Villanueva Pedraza, E., Fernandez Villarroel, R.A. (2025). Magnetic Field Penetration Depth in Various Materials and Applications. *Appl. Sci.* 15 (4), 2225. https://doi.org/10.3390/APP15042225.

Avci, U., Güleç, A. (2021). Effect of Different Sintering Temperatures on Microstructure and Mechanical Properties for Pure Al Material Produced by Powder Metallurgy. *El-Cezeri* 8 (1), 462–470. https://doi.org/10.31202/ecjse.789587.

Bao, R., Yi, J.H., Peng, Y.D., Li, F.X., Li, S., Li, S.Y. (2022). Skin effect of WC–8 wt% Co alloy by microwave sintering. *Rare Met.* 41(4), 1364–1368. https://doi.org/10.1007/s12598-015-0488-3.

Borges, O.H., Cardoso, A.L.F., Moreira, M.H., Klein-Gunnewiek, R.F., Pandolfelli, V.C. (2023). Conventional and microwave-assisted sintering of ZnO-containing CAC-bonded alumina-based refractory castables. *J. Eur. Ceram. Soc.* 43 (14), 6562–6570. https://doi.org/10.1016/j.jeurceramsoc.2023.06.063.

Çavdar, U. (2014). Mechanical properties of hot forged ANS11050 steel. *Mater. Test.* 56 (3), 208–212. https://doi.org/10.3139/120.110555.

Çavdar, U., Atik, E. (2014). Investigation of conventional-and induction-sintered iron and iron-based powder metal compacts. *JOM* 66 (6), 1027–1034. https://doi.org/10.1007/S11837-014-0977-0.

Çavdar, U., Gülşahin, I. (2014). Ultra high frequency induction welding of powder metal compacts. *Rev. Metal.* 50 (2), e016. https://doi.org/10.3989/revmetalm.016.

Cavdar, U., Atik, E., Akgul, M.B. (2014). Magnetic-Thermal Analysis and Rapid Consolidation of FE–3 wt.% CU Powder Metal Compacts Sintered by Medium-Frequency Induction-Heated System. *Powder Metall. Met. Ceram.* 53 (3–4), 191–198. https://doi.org/10.1007/S11106-014-9603-5.

Çavdar, P.S., Çavdar, U. (2015). The evaluation of different environments in ultra-high frequency induction sintered powder metal compacts. *Rev. Metal.* 51 (1), e036. https://doi.org/http://dx.doi.org/10.3989/revmetalm.036.

Chang, R., Wang, Y., Zang, J., Yu, Y., Lu, J., Xu, X. (2017). Investigation of Ti coatings on cubic boron nitride (cBN) grits by discharge treatment in spark plasma sintering system. *Adv. Powder Technol.* 28 (9), 2281–2287. https://doi.org/10.1016/J.APT.2017.06.008.

Durmuş, H., Gül, C., Çömez, N., Uzun, R. (2020). From metal chips to composite: Effect of age-hardening on mechanical and wear properties of Al_2O_3 reinforced AA7075 composites. *Sci. Sinter.* 52 (2), 177–186. https://doi.org/10.2298/SOS2002177D.

Dwivedi, S.P., Chaudhary, V., Sharma, S. (2024). Synergistic performance evaluation of copper–WC-graphene composites: Microstructure, mechanical properties, corrosion, and wear behavior under microwave sintering. *Mater. Chem. Phys.* 317, 129202. https://doi.org/10.1016/j.matchemphys.2024.129202.

Elkilani, R.H.R., Çuğ, H., Erden, A.M. (2024). The effects of hot rolling process on mechanical properties, corrosion resistance, and microstructures of Mo-Ni alloyed steels produced by powder metallurgy. *Sci. Sinter.* 56 (1), 59–78. https://doi.org/10.2298/SOS230625040E.

Fei, H., Wu, H., Yang, X., Xing, B., Yang, Y., Xiong, J., Liu, J. (2021). Sintering of the WC-6%Co cemented carbides for improved mechanical and cutting performance using Micro-FAST. *Int. J. Refract. Hard Met.* 98, 105545. https://doi.org/10.1016/J.IJRMHM.2021.105545.

Fu, L., Yue, J., Liu, W., Han, Z., Bai, D., Xu, G. (2023). Analysis and experiment of sintering and densification of magnesia particles. *Chem. Eng. Sci.* 268, 118396. https://doi.org/10.1016/j.ces.2022.118396.

Furlan, K.P., Pasquarelli, R.M., Krekeler, T., Ritter, M., Zierold, R., Nielsch, K., Schneider, G.A., Janssen, R. (2017). Highly porous α-Al_2O_3 ceramics obtained by sintering atomic layer deposited inverse opals. *Ceram. Int.* 43 (14), 11260–11264. https://doi.org/10.1016/j.ceramint.2017.05.176.

Gafur, M.A., Ahmed, A.F., Abrar, R., Soshi, S.S. (2023). Development and Characterization of Aluminium-Based Metal Matrix Composites. *JMSA* 14 (1), 1–19. https://doi.org/10.4236/MSA.2023.141001.

Ge, W., Wu, B., Wang, S., Xu, S., Shang, C., Zhang, Z., Wang, Y. (2017). Characterization and properties of CuZrAlTiNi high entropy alloy coating obtained by mechanical alloying and vacuum hot pressing sintering. *Adv. Powder Technol.* 28 (10), 2556–2563. https://doi.org/10.1016/J.APT.2017.07.006.

Ghobadi, H., Ebadzadeh, T., Sadeghian, Z., Barzegar-Bafrooei, H., Nemati, A. (2017). Microwave-assisted sintering of Al_2O_3-MWCNT nanocomposites. *Ceram. Int.* 43 (8), 6105–6109. https://doi.org/10.1016/j.ceramint.2017.02.003.

Gokozan, H., Tastan, M., Taskin, S., Cavdar, P.S., Cavdar, U. (2016). Comparison of electrical energy consumption for different material processing procedures. *Mater. Test.* 58 (11–12), 1009–1013. https://doi.org/10.3139/120.110954.

Gül, B., Gezici, L.U., Ayvaz, M., Çavdar, U. (2020). The comparative study of conventional and ultra-high frequency induction sintering behavior of pure aluminum. *Int. Adv. Res. Eng. J.* 4 (3), 173–179. https://doi.org/10.35860/iarej.729395.

Jeong, K., Tatami, J., Iijima, M., Nishimura, T. (2017). Spark plasma sintering of silicon nitride using nanocomposite particles. *Adv. Powder Technol.* 28 (1), 37–42. https://doi.org/10.1016/J.APT.2016.06.027.

Junqueira, L.A., Tabriz, A.G., Garg, V., Kolipaka, S.S., Hui, H.W., Boersen, N., Roberts, S., Jones, J., Douroumis, D. (2025). Selective laser sintering for printing bilayer tablets. *Int. J. Pharm.* 670, 125116. https://doi.org/10.1016/J.IJPHARM.2024.125116.

Kozhakhmetov, Y., Skakov, M., Mukhamedova, N., Kurbanbekov, S., Ramankulov, S., Wieleba, W. (2021). Changes in the microstructural state of Ti-Al-Nb-based alloys depending on the temperature cycle during spark plasma sintering. *Mater. Test.* 63 (2), 119–123. https://doi.org/10.1515/MT-2020-0017.

Leszczyńska-Madej, B., Garbiec, D., Madej, M. (2019). Effect of sintering temperature on microstructure and selected properties of spark plasma sintered Al-SiC composites. *Vacuum* 164, 250–255. https://doi.org/10.1016/J.VACUUM.2019.03.033.

Lu, C., Yang, J., Zhao, Y., Lei, X., Huang, J., Chen, S., Ye, Z. (2021). Influence of applied electric field on atom diffusion behavior and mechanism for W/NiFe interface in diffusion bonding of Steel/NiFe interlayer/W by spark plasma sintering. *Appl. Surf. Sci.* 541, 148516. https://doi.org/10.1016/J.APSUSC.2020.148516.

Mishra, R. (2021). *Synthesis of Materials by Induction Heating. In Handbook on Synthesis Strategies for Advanced Materials*. Tyagi, A.K., Ningthoujam, R.S. (Eds), Indian Institute of Metals Series. Springer, Singapore, pp. 215–228. https://doi.org/10.1007/978-981-16-1807-9_8

Mohammadi, M., Coppola, B., Montanaro, L., Palmero, P. (2023). Digital light processing of high-strength hydroxyapatite ceramics: Role of particle size and printing parameters on microstructural defects and mechanical properties. *J. Eur. Ceram. Soc.* 43 (7), 2761–2772. https://doi.org/10.1016/j.jeurceramsoc.2022.11.047.

Nisar, A., Zhang, C., Boesl, B., Agarwal, A. (2021). Unconventional Materials Processing Using Spark Plasma Sintering. *Ceramics* 4 (1), 20–39. https://doi.org/10.3390/ceramics4010003.

Özdemir, A., Taştan, M. (2014). PLL based digital adaptive filter for detecting interharmonics. *Math. Probl. Eng.* ID 01781, 10 p ages. https://doi.org/10.1155/2014/501781.

Ozer, M., Kaplan, Y., Özer, A., Aksoz, S. (2024). Influence of different sintering techniques on the wear properties of Al-15Si-2.5Cu-0.5Mg/B4C composites. *Sci. Sinter.* 56 (3), 60–60. https://doi.org/10.2298/SOS231003060O.

Pan, K., Liu, X., Wang, B., Gao, S., Wu, S., Li, N. (2024). The rapid densification behavior of powder metallurgy Ti alloys by induction heating sintering. *J. Mater. Sci. Technol.* 181, 152–164. https://doi.org/10.1016/J.JMST.2023.10.009.

Parasuraman, P., Sonar, T., Rajakumar, S. (2022). Microstructure, tensile properties and fracture toughness of friction stir welded AA7075-T651 aluminium alloy joints. *Mater. Test.* 64 (12), 1843–1850. https://doi.org/10.1515/MT-2022-0212.

Raihanuzzaman, R.M., Han, S.T., Ghomashchi, R., Kim, H.S., Hong, S.J. (2015). Conventional sintering of WC with nano-sized Co binder: Characterization and mechanical behavior. *International Int. J. Refract. Met. Hard Mater.* 53, 2–6. https://doi.org/10.1016/j.ijrmhm.2015.04.033.

Reddy, M.P., Ubaid, F., Shakoor, R.A., Parande, G., Manakari, V., Mohamed, A.M.A., Gupta, M. (2017). Effect of reinforcement concentration on the properties of hot extruded Al-Al_2O_3 composites synthesized through microwave sintering process. *Mater. Sci. Eng. A* 696, 60–69. https://doi.org/10.1016/j.msea.2017.04.064.

Rochala, P., Hofmann, C., Kroll, M., Panhale, S., Javed, R., Hiller, K. (2023). Inductive Sintering of Silver Micro Particles for Bonding of Microelectronic Components. *Electronics* 12 (15), 3247. https://doi.org/10.3390/ELECTRONICS12153247.

Rojas-Macedo, F.J., Teutle-Coyotecatl, B., Contreras-Bulnes, R., Rodríguez-Vilchis, L.E., Reyes-Cervantes, E., Velazquez-Enriquez, U. (2024). Effect of polymerization methods on surface roughness and hardness of commercially available self-curing acrylic resins: a comparative study. *Pigment Resin Technol.* 54 (4), 540-548. https://doi.org/10.1108/PRT-12-2023-0120.

Ruiz-Esparza-Rodríguez, M.A., Garay-Reyes, C.G., Mendoza-Duarte, J.M., Estrada-Guel, I., Hernández-Rivera, J.L., Cruz-Rivera, J.J., Gutiérrez-Castañeda, E., González, S., Garay-Tapia, A.M., Martínez-Sánchez, R. (2022). Evaluation of high-frequency induction heat

sintering and conventional sintering in AlxCoCrFeMnNi high-entropy alloys. *J. Alloys Compd*. 910, 164780. https://doi.org/10.1016/j.jallcom.2022.164780.

Singh, D.K. (2021). *Mechanical Testing of Materials*. In *Strength of Materials*. pp. 857–866. Springer Cham. https://doi.org/10.1007/978-3-030-59667-5_18.

Taskin, S., Gokozan, H. (2011). Determination of the Spectral Properties and Harmonic Levels for Driving an Induction Motor by an Inverter Driver under the Different Load Conditions. *Electrical Engineering* 108 (2), 75–80. https://doi.org/10.5755/j01.eee.108.2.149.

Taştan, M. (2019). Adaptive Notch Filter Bank Based Power Quality Analysis of an Ultra-High Frequency Induction Heating System. *Balkan J. Electr. Comput. Eng* 7 (2), 131–136. https://doi.org/10.17694/bajece.498021.

Taştan, M., Gökozan, H., Taşkin, S., Çavdar, U. (2015). Comparative energy consumption analyses of an ultra high frequency induction heating system for material processing applications. *Rev. Metal.* 51 (3), e046. https://doi.org/10.3989/revmetalm.046.

Taştan, M., Gökozan, H., Çavdar, P.S., Soy, G., Çavdar, U. (2020). Cost analysis of T6 induction heat treatment for the aluminum-copper powder metal compacts. *Sci. Sinter.* 52 (1), 77–85. https://doi.org/10.2298/SOS2001077T.

Teker, T., Yllmaz, S.O., Karakoca, A. (2023). Improvement of metallurgical properties of A356 aluminium alloy by AlCrFeSrTiBSi master alloy. *Mater. Test.* 65 (2), 224–232. https://doi.org/10.1515/mt-2022-0407.

Teslia, S.Y., Kucher, O.S., Bogomol, I.I., Loboda, P.I., Solodkyi, I.V. (2024). Induction Zone Sintering of WC–8Co Hard Alloy. *Mater. Sci.* 59 (5), 638–643. https://doi.org/10.1007/S11003-024-00821-7.

Varela De Seijas, M.O., Bardenhagen, M., Rohr, T., Stoll, E. (2023). Indirect Induction Sintering of Metal Parts Produced through Material Extrusion Additive Manufacturing. *Materials* 16 (2), 885. https://doi.org/10.3390/ma16020885.

Velavan, K., Mohan, B., Anbuchezhiyan, G., Senthilkumar, N. (2021). Implications of SiC/Al_2O_3 Reinforced Al-Mg-Zn Alloy Hybrid Nano Composites Using Vacuum Sintering Method. *Silicon* 13 (10), 3639–3647. https://doi.org/10.1007/s12633-020-00928-x.

Vilchez, N., Ortega Varela de Seijas, M., Bardenhagen, A., Rohr, T., Stoll, E. (2023). A Novel Induction Heater for Sintering Metal Compacts with a Hybrid Material Extrusion Device. *Electronics* 12 (14), 3033. https://doi.org/10.3390/electronics12143033.

Wu, J., Wu, X., Gao, Y., Yan, Z. (2024). Innovations in Electric Current-Assisted Sintering for SOFC: A Review of Advances in Flash Sintering and Ultrafast High-Temperature Sintering. *Appl. Sci.* 14 (10), 3953. https://doi.org/10.3390/app14103953.

Yang, H., Zhou, X., Yu, J., Wang, H., Huang, Z. (2016). Microwave and conventional sintering of the SiC/SiC composites: The densification and pore distributions. *J. Alloys Compd.* 662, 252–258. https://doi.org/10.1016/j.jallcom.2015.12.085.

Zuo, F., Wu, R.D., Zhan, L. H., Deng, Y.N., Grasso, S., Chen, X.L., Lin, H.T. (2025). Scalable and efficient consolidation of Al_2O_3 and SiC ceramics using a powder medium-based ultrafast high-temperature sintering (P-UHS). *Scri. Mater.* 266, 116768. https://doi.org/10.1016/j.scriptamat.2025.116768.